Zhong *et al. Chem. Biol. Technol. Agric.* (2023) 10:140
https://doi.org/10.1186/s40538-023-00510-8

Chemical and Biological Technologies in Agriculture

RESEARCH

Open Access

Enhancing the salt stress resistance of seeds and seedlings via a brassinolide sustained release agent system

Ximing Zhong[1], Ruopeng Lan[1], Guofeng Su[1], Li Hao[1], Hua Xu[1], Hongjun Zhou[1*] and Xinhua Zhou[1*]

Abstract

Background The growing escalation of soil salinization is tremendously threatening the global food security and the development of sustainable agriculture. To address the worldwide predicament caused by salt stress toward crops, combining nanotechnology with the merits of plant hormone may become an efficient and effective approach.

Results In this work, a sustained release agent system (BR@MSN) was developed by loading brassinolide (BR) to mesoporous silica nanoparticles (MSN) to enhance the salt stress resistance of cucumber seeds and seedlings. The obtained BR@MSN agent was about 120 nm. As an endogenous plant hormone, promotion in crop growth was found at low BR concentration. Due to the sustained release property, BR@MSN avoided excessive BR exposure to seeds and seedlings to cause inhibitory effects. After the soil application of BR@MSN, the promotion effect from BR combined with the regulation enhancement from MSN nanocarrier improved the seed germination rate by 11.76% under saline environment. Compared with the same BR concentration (2.0 mg/L), BR@MSN increased the seed germination rate even by 1324.29%. In addition, remarkable wettability on foliar surfaces was found, and the foliar application of BR@MSN significantly enhanced the salt stress resistance of cucumber seedlings by alleviating the accumulation of reactive oxygen species (ROS) and increasing the cell viability along with the improvement in superoxide dismutase (SOD) activity (234.11%), the decrease in malondialdehyde (MDA) content (61.30%), and the increase in chlorophyll content (110.88%).

Conclusions The newly developed BR@MSN agents could effectively enhance the salt stress resistance of crop seeds and seedlings, and their applications significantly improved the seed germination rate and seedling growth. The remarkable efficacy makes this BR@MSN agent system potential in agricultural field for enhancing the salt stress resistance of crops and facilitating the development of sustainable agriculture.

Keywords Salt stress resistance, Brassinolide, Mesoporous silica nanocarriers, Sustained release, Seed germination, Seedling growth

*Correspondence:
Hongjun Zhou
hongjunzhou@163.com
Xinhua Zhou
cexinhuazhou@163.com
Full list of author information is available at the end of the article

Graphical Abstract

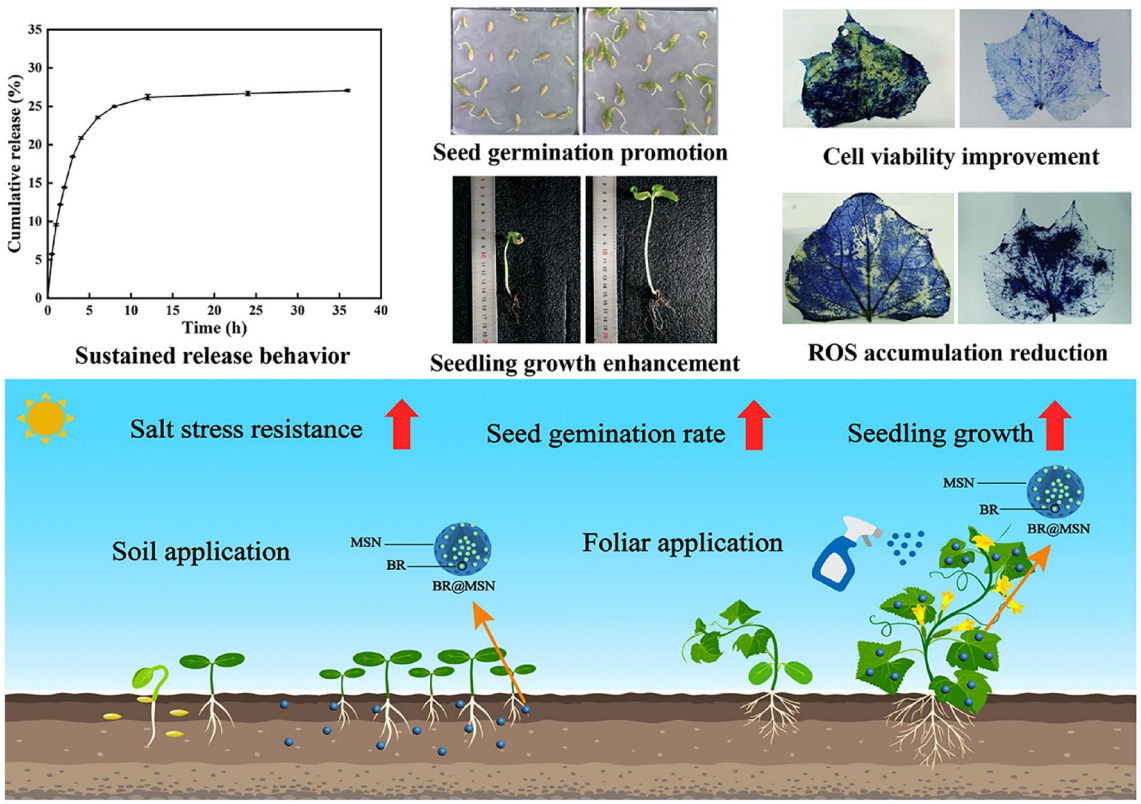

Introduction

Soil salinization is a worldwide challenge that tremendously threatens global food security and sustainable agriculture [1–3]. In the world, about 800 million hectares of arable lands are affected by soil salinization, and the total saline land even reaches 1125 million hectares [4, 5]. However, plants cannot grow up normally in the soil with high salt content due to the occurrence of salt stress exerting adverse effects on seed germination, growth, flowering, and fruiting [6]. When plants are suffered from salt stress, the intake of water and nutrients will be reduced [7]. The water shortage and nutrients deficiency induce osmotic stress and ionic stress, which further leads to the occurrence and accumulation of reactive oxygen species (ROS) [8–10]. Excessive accumulation of ROS in cells destroys the normal physiological and molecular function of cells, leads to metabolic disorder, and thus brings about oxidative damages [11–14]. In the meanwhile, salt stress adversely affects the photosynthesis of plants, along with the reduction in available resources and the inhibition in cell division, thus impeding the plant growth and development [15, 16]. As we know, cucumber is a healthy vegetable enriched with vitamins, fibers, and nutritional elements, and it can be used for maintaining blood pressure, detoxifying body, and preventing cancer [17]. Due to the high nutritional, medicinal and health beneficial values, cucumber is economically important and become the top ten vegetables produced globally [18]. However, cucumber plants are susceptible to saline environment, and the occurrence of salt stress will result in serious yield reduction, which will aggravate the instability of global food supply [19]. Therefore, seeking an effective approach to enhancing the salt stress resistance of cucumber plants is highly urgent.

Plant hormones are well-known to enhance the resistance of plants against biotic and abiotic stresses, and thus potential for alleviating the salt stress. Brassinosteroids, recognized as the sixth kind of plant hormones, are polyhydroxysterols with high physiological activity [20–22]. Since brassinolide (BR) was first isolated from rape pollen in 1979, more than 70 brassinosteroid derivatives and conjugates have been found and identified from various plants [23–25]. Among brassinosteroid derivatives and

conjugates, BR possesses the most biological activity, and generally regarded as an efficient, broad-spectrum, and non-toxic plant growth regulator, regulating seed germination, flowering and other growth stages, playing important role in the growth and development of plants [26–28]. In addition, BR is able to improve antioxidant system and enhance the tolerance of plants against various environmental stresses, inducing plants to resist abiotic stresses, including the salt stresses [29–32]. However, in agricultural applications, compared with foliar spraying, soil application of BR generally causes the fixation by soil or the loss of active components, leading to the decrease in utilization efficacy. At the same time, due to the endogenous property, BR is easy to be metabolized, which seriously affects the duration of physiological effects in plants, and excessive active components are necessarily employed to maintain the efficacy. However, excessive application of BR is potential to inhibit plant growth [28, 33]. Therefore, appropriate methods are urgently seeking to improve the utilization efficacy and duration of BR to enhance the salts stress resistance of plants.

As we know, nanotechnology has been applied to theoretical research and practical applications in many fields [34–37]. Until recent years, many emerging technologies have been integrated into agricultural field, and the applications of nanomaterials and technologies has turned to agricultural field to achieve sustainable agriculture [38–40]. Among them, mesoporous silica nanoparticles (MSN) attract worldwide attention due to the unique merits in tailored structures, remarkable surface area, easy surface-functionalization feature, good biocompatibility, and cost-effectiveness [41–43]. Of note, MSN has been widely utilized in agricultural field as a nanocarrier to protect pesticides from photodegration and prolong pest control. Zhong et al. revealed the zein-functionalized MSN nanocarriers exhibited high pesticide loading capacity, and the obtained nanopesticides also demonstrated enhanced photostability and controlled release behavior [44]. Shen et al. found the polydopamine-modified MSN effectively controlled the release rate of avermectin, thus prolonging the duration of pesticide and reducing detrimental environmental hazards [45]. Zhao et al. designed a pesticide-loaded MSN system and investigated the translocation and distribution of MSN in cucumber plants [46]. The results showed that the uptake of MSN by cucumber leaves could be achieved. In addition, many researches revealed the supplement of Si provided by silica is beneficial to the water-use efficiency of the plants under salt stress and thus improved plant growth [47, 48]. Therefore, considering the features of MSN and BR, employing MSN as nanocarrier to load BR may become a feasible strategy to address the dilemma caused by salt stress.

In this work, a brassinolide (BR) sustained release agent system (BR@MSN) were developed by loading BR to MSN nanocarrier, and the nanocarrier was synthesized via the hydrolysis and condensation of tetraethyl orthosilicate (TEOS) under alkaline condition using cetyl trimethyl ammonium bromide (CTAB) as a template. The successful preparation of BR@MSN was confirmed by Fourier Transform Infrared (FTIR) and thermogravimetric (TG) characterizations, and the morphology was observed via scanning electron microscopy (SEM). The as-obtained BR@MSN demonstrated sustained release behavior, and such behavior avoided excessive BR exposure causing inhibitory effects on cucumber seed germination and plant growth. Besides, the collaboration of the sustained release of BR from BR@MSN and the regulation enhancement from MSN significantly improved the cucumber seed germination rate and stem elongation under saline condition. Of note, these BR sustained release agents exhibited remarkable wettability on foliar surfaces, and the foliar application of BR@MSN was able to enhance the salt stress resistance of cucumber seedlings by reducing the accumulation of reactive oxygen species and enhancing the cell viability. Therefore, these newly developed BR sustained release agents are conducive to the seed germination and seedling growth under adverse environment, and they are potential for alleviating the worldwide predicaments caused by salt stress. The synthetic route of BR@MSN and their enhancement in the salt stress resistance toward cucumber seeds and seedlings are demonstrated in Fig. 1.

Materials and methods

Experimental materials

Tetraethyl orthosilicate (TEOS, 98%), cetyl trimethyl ammonium bromide (CTAB, 99%), hydrochloric acid (37%), thiobarbituric acid (TBA, 98%), trichloroacetic acid (TCA, 99%), brassinolide (BL, ≥ 90%), sodium hypochlorite solution (6.0%), naphthylboronic acid (97%), acetonitrile (HPLC), disodium ethylenediaminetetraacetate (DETA-Na_2, 0.1 mol/L), D-methionine (Met, 99%), riboflavin (98%), and pyridine (99.8%) were purchased from Aladdin. Nitroblue tetrazolium (NBT, 98%), Evans blue (0.5%), and phosphate buffer solution (0.1 mol/L, pH = 7.0) were procured from Beijing Reagan Biotechnology Co., Ltd. Sodiun chloride (NaCl, 99.5%), lactic acid (90%) and glycerol (99%) were provided by Macklin. Silwet L-77 was provided by Beijing Solarbio Technology Co., Ltd. Absolute ethanol and ammonia solution (25%) were purchase from Tianjin Damao Chemical Reagent Factory. Nutrient soil was provided by Shandong Shouhe Seed Industry Co., Ltd. Vermiculite was bought from

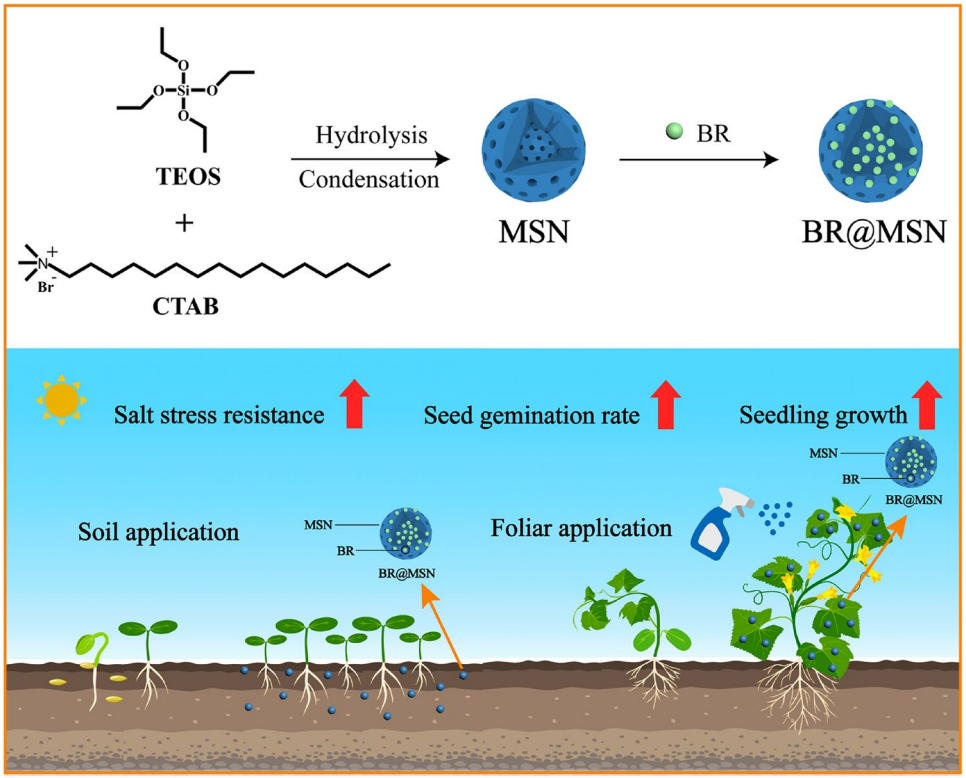

Fig. 1 **a** Synthetic route of BR@MSN. **b** Applications of BR@MSN enhanced the salt stress resistance toward cucumber seeds and seedlings

Xinyang Guotong E-commerce Co., Ltd. All chemicals were used as received without further purification.

Synthesis of mesoporous silica nanoparticle (MSN) nanocarriers

The method to synthesize MSN nanocarriers was adopted according to previous report [45]. First, 0.45 g CTAB was mixed with 180 mL ethanol aqueous solution (concentration of 16.7%) in a 250 mL flask, and 4.00 mL ammonia solution (25%) was added. After stirring for 30 min at 70 ℃, 1.50 mL TEOS was added dropwise into above solution, and the reaction proceeded for 24 h. Afterward, the obtained solution was cooled down to room temperature, and then centrifuged at 12,000 rpm for 7 min. The supernatant was discarded, and the precipitate was washed with ethanol and water trice to remove the residual reactants. Subsequently, methanol solution containing 0.5% hydrochloric acid was utilized to wash the crude product overnight to remove CTAB. After drying at 60 ℃, MSN nanocarriers were obtained.

Preparation of the BR sustained release agents (BR@MSN)

BR sustained release agents (BR@MSN) were prepared by loading BR to MSN nanocarriers. Similar to previous report [49], 5.00 mg brassinolide was placed into a 100 mL brown conical flask, and then 50.0 mL anhydrous ethanol was added to prepare a brassinolide solution with a concentration of 0.1 mg/mL. Afterward, 0.10 g MSN was added into above solution, and the mixture was shaken at 25 ℃ for 24 h. Subsequently, the mixture was centrifuged at 12,000 rpm for 20 min. The supernatant was discarded, and the precipitate was dried at room temperature to obtain BR@MSN. The synthetic route of BR@MSN is demonstrated in Fig. 1.

Determination of seed germination rate

Seed germination rate could be determined using the method reported by Khan [50]. Uniform cucumber seeds were selected and disinfected with sodium hypochlorite solution (1.0%) for 10 min. Afterward, deionized water was used to rinse the treated seeds for 5 min and then dried at room temperature. The dried cucumber seeds were placed in a 50.0 mL tube and mixed with the sample (BR, MSN, and BR@MSN, respectively) dispersion with different BR concentrations (0.125 mg/L, 0.25 mg/L, 0.5 mg/L, 1.0 mg/L, and 2.0 mg/L, respectively). Specifically, the BR@MSN concentration indicated the inherent BR concentration, and the mass of MSN used for experiment was the same with BR@MSN. Above tubes

were further shaking in dark condition for 8 h before the treated cucumber seeds were placed in a germinating box (dimension of 10.0 cm × 10.0 cm × 5.0 cm, 30 seeds in each box) with 10.0 mL NaCl aqueous solution (150 mM). The cucumber seeds were cultured for 7 days under saline condition. The germination rate (*GR*) of cucumber seeds could be calculated using the following equation:

$$GR = \frac{N}{S} \times 100\% \quad (1)$$

where N and S are the number of germinated seeds and the total number of tested seeds, respectively.

Plant growth evaluation

Similar to Li's work [51], to evaluate the effect of BR concentrations on the growth of cucumber seedlings, cucumber seeds were sown in soil mix (commercial nutrient soil and vermiculite, 3:1 v/v) and watered with 0.3 mL sample (BR, MSN, BR@MSN, respectively) dispersion with different BR concentrations (0.125 mg/L, 0.25 mg/L, 0.5 mg/L, 1.0 mg/L, and 2.0 mg/L, respectively) every 5 days. The commercial nutrient soil was consisted of organic matter, humic acid, perlite, and coconut bran. During the growth stage, seedlings were grown in growth room with the following settings: 24 ± 1 ℃ (day time) and 21 ± 1 ℃ (night time), 14/10 h as the day/night regime, 60% relative humidity. No pesticide or other fertilizer was used during the plant growth. Seedling growth status was recorded by taking photos after 15 culturing days.

Determination of cell viability and superoxide anion (O^{2-}) content

The methods to determine cell viability and superoxide anion (O^{2-}) content of cucumber seedlings are similar to the previous work [52]. The cucumber seedlings with three real leaves were transplanted to the bottles filled with water. Afterward, the cucumber seedlings were treated by dropping different sample (BR@MSN, MSN, and BR) dispersions with different BR concentrations (0.125 mg/L, 0.25 mg/L, 0.5 mg/L, 1.0 mg/L, and 2.0 mg/L, respectively) on the second leaf. After culturing for 24 h, the water in bottles were changed to NaCl solution (120 mM). After additional 24 h, cucumber leaves were cut and stained in Evan blue solution (5%) in dark for 6 h to determine the cell viability. To determine superoxide anion (O^{2-}) content, the cucumber leaves were soaked in 100 mmol/L phosphate buffer solution (with 5 mg/mL NBT) for staining for 6 h. Afterward, the stained leaves were taken out, rinsed with water, and then immersed in a decolorizing solution (ethanol:lactic acid:glycerol = 3:1:1) at 95 ℃ to completely remove the chlorophyll. The treated leaves were recorded by taking photos for comparison.

Determination of superoxide dismutase (SOD) activity

The SOD activity could be determined according to previous report [49]. First, 1.0 g cucumber leaves and 4.0 mL phosphate buffer solution were mixed and then ground in a precooled mortar. Furthermore, the ground mixture was centrifuged (4000 rpm for 10 min). The supernatant was diluted to 10.0 mL using phosphate buffer solution, and the diluted solution was served as enzyme solution. To determine SOD activity, 0.05 mL above enzyme solution was mixed with 1.5 mL 0.05 mol/L phosphate buffer solution, 0.3 mL 100 μmol/L EDTA–Na_2 solution, 0.3 mL 20 μmol/L riboflavin, 0.3 mL 750 μmol/L NBT, 0.3 mL 130 mmol/L Met solution, and 0.25 mL deionized water. After suffering from a sunlight lamp for 20 min, the absorbance of the treated sample was measured by a UV-3600 Plus spectrophotometer (Shimadzu, Japan) at 560 nm. The sample placing in dark was served as a control group. SOD content could be determined using the following equation:

$$\mathrm{SOD} = 2 \times V_T \times (A_{CK} - A_E)/(A_{CK} \times m \times V_s) \quad (2)$$

where A_{CK} is the absorbance of control group, A_E is the absorbance of the treated sample, m corresponds to the mass of cucumber leaves, V_T represents the total volume of sample solution, V_S represents the volume of test sample.

Determination of malondialdehyde (MDA) content

To determine MDA content, previous method was adopted [53]. Specifically, 0.5 g cucumber leave was added in a pre-cooled bowl grinding with 5.0 mL TCA (5.0%), and then centrifuged in a refrigerated centrifuge at a speed of 3000 rpm for 10 min to obtain the supernatant MDA extract. Afterward, 2.0 mL extract was transferred to a tube and mixed with 2.0 mL TBA (0.67%). The mixture was boiling in water for 30 min. After cooling down to room temperature, the mixture was centrifuged, and the supernatant was used for absorbance measurement. The absorbances of the samples at 450 nm, 532 nm, and 600 nm were determined by a UV-3600 Plus spectrophotometer. The calculation for MDA content could be employed as the following equation:

$$\mathrm{MDA} = (6.45 \times (A_{532} - A_{600}) - 0.56 \times A_{450}) \times V_2 \times V/(m \times V_1 \times 1000) \quad (3)$$

where V is the total extract volume, m is the mass of cucumber leaves, V_1 is the extract volume for test, and V_2 is the total volume of the solution for absorbance measurement.

Determination of Chlorophyll Content

The chlorophyll content could be determined according to previous work [53]. First, 0.2 g cucumber leaves were ground and then mixed with 10.0 mL acetone (80%), and the mixture was stored in dark with shaking for 24 h at room temperature. Acetone (80%) was served as a blank control, and the absorbances of the samples were measured at the wavelengths of 645 nm and 663 nm. The contents of chlorophyll a (C_a), chlorophyll b (C_b), and total chlorophyll (C_T) could be, respectively, calculated according to Eqs. (4–6):

$$C_a = 12.72 \times A_{663} - 2.59 \times A_{645} \quad (4)$$

$$C_b = 22.88 \times A_{645} - 4.67 \times A_{633} \quad (5)$$

$$C_T = C_a + C_b \quad (6)$$

where C_a, C_b, and C_T are the contents of chlorophyll a, chlorophyll b, and total chlorophyll, respectively.

Investigation of sustained release behavior

To investigate the sustained release behavior of BR from BR@MSN, 5.0 mg BR@MSN was dispersed in 5.0 mL ethanol solution (60%), and then was added into a dialysis bag (5000 Da), which was placed in a brown conical flask with 25 mL ethanol solution (60%) used as the release medium. Above flask was shaken at 25℃. Afterward, 1.0 mL release medium was taken out at a certain interval, and 1.0 mL ethanol solution (60%) was replenished in the flask. The release medium (1.0 mL) taken out from flask was mixed with 1.0 mL naphthylboronic acid solution (0.4 mg/mL in pyrine), and the absorbance of above solution was measure at 290 nm by a high-performance liquid chromatography (HPLC). In detail, the mobile phase employed for HPLC measurement was acetonitrile:water = 85:15. BR concentration could be calculated according to the standard curve of A = 1857.77228C + 756.14428 (R^2 = 0.999). The cumulative release rate (R_i) of BR@MSN could be calculated by the following equation [49]:

$$R_i = \begin{cases} C_i \times 0.03/m_{BR} (i = 1) \\ C_i \times 0.03/m_{BR} + \sum_{i=1}^{i-1} C_i \times 0.001/m_{BR} (i > 1) \end{cases} \quad (7)$$

where C_i is the BR concentration at different intervals, while m_{BR} represents the total mass of BR in the samples.

Statistical analysis

The statistical analysis was performed using a IBM SPSS software (24.0 version). The experimental data were measured in three replicates, and the significant differences in means were compared using Duncan's test at a significant level of $P \leq 0.05$ [54].

Characterizations

To analyze the chemical structures of BR, MSN, and BR@MSN, Fourier Transform Infrared (FTIR) spectra were recorded using a Spectrum 100 (Perkin-Elmer, USA) in the wavenumbers ranging from 4000 cm^{-1} to 450 cm^{-1}. Besides, a TGA 2 thermogravimetric analyzer (Mettler-Toledo, Switzerland) was employed to analyze the thermal stability of BR, MSN, and BR@MSN. The experimental temperature was set from 40 ℃ to 800 ℃ with a heating rate of 10 ℃/min, and the whole heating process was under N_2 atmosphere with a flowing rate of 50 mL/min. The contact angles of various droplets on cucumber foliar surfaces were determined by a contact angle meter (Theta, Biolin). The hydrodynamic sizes of samples were determined using a 90 Plus PALS particle size analyzer (Bruker, USA). In addition, a HD scanning electron microscopy (ZEISS, Germany) was employed to compare the morphologies of MSN and BR@MSN.

Results and discussion

Chemical structure confirmation

To confirm the successful preparation of BR@MSN, FTIR analysis was utilized. The FTIR spectra of BR, MSN, and BR@MSN are shown in Fig. 2a. In the spectrum of MSN, the peaks at 465 cm^{-1}, 799 cm^{-1}, and 1093 cm^{-1} were, respectively, ascribed to the bending vibration, symmetric stretching vibration, and asymmetric stretching vibration of Si–O–Si [55]. Besides, the peaks at 961 cm^{-1} and 3439 cm^{-1} corresponded to the bending vibration and stretching vibration of Si–OH. Above results revealed the successful synthesis of MSN. As for BR spectrum, the peaks at 1458 cm^{-1}, 2868 cm^{-1}, and 2964 cm^{-1}, respectively, represented the bending vibration, symmetric stretching vibration, and asymmetric stretching vibration of $-CH_2-$ structure. In addition, the peaks at 1728 cm^{-1} and 3395 cm^{-1} were attributed to the stretching vibration of ester groups and the absorption peak of hydrogen

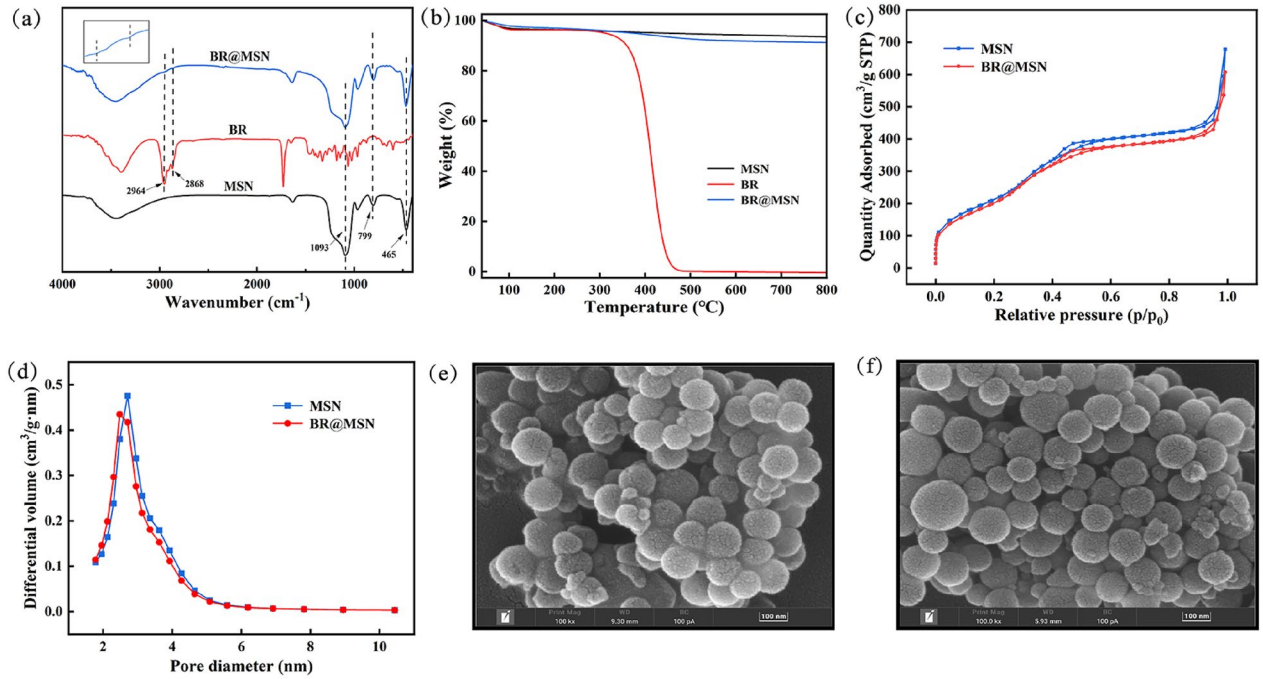

Fig. 2 **a** FTIR spectra and **b** TG curves of BR, MSN, and BR@MSN. **c** Nitrogen adsorption–desorption isotherms and **d** pore size distributions of MSN and BR@MSN. SEM images of **e** MSN and **f** BR@MSN

groups. Of note, the characteristic peaks of MSN and BR could be found in the spectrum of BR@MSN, which confirmed the successful preparation of BR@MSN.

Thermal stability analysis

It is well-known that organic components are easier to decompose compared with inorganic materials along with the increase in temperature. Therefore, the loading of BR in MSN will give rise to the discrepancy in thermal stability. Figure 2b and Additional file 1: Fig. S1 show the thermogravimetric (TG) and derivative thermogravimetric (DTG) curves of BR, MSN, and BR@MSN, respectively. The weight loss before 120 ℃ was mainly due to water evaporation [55]. Besides, at the temperature ranging from 120 ℃ to 800 ℃, the weight loss rates of MSN and BR@MSN were 3.29% and 6.90%, respectively, implying the loading rate of BR in BR@MSN was about 3.61%. Specifically, as for BR, it began to decompose at 280 ℃, and the main weight loss stage was located at 413 ℃. Before 500 ℃, BR was completely decomposed. In the case of BR@MSN, an obvious weight loss peak was found at 428 ℃ (Additional file 1: Fig. S1), which was mainly attributed to the decomposition of BR in BR@MSN. The main decomposition temperature of BR shifting from 413 ℃ to 428 ℃ was due to the presence of MSN to some degree insulating the heat, reflective of the improvement in thermal stability [56]. Therefore, aside from FTIR analysis, above results also confirmed the successful loading of BR in MSN, and BR@MSN exhibited enhanced thermal stability.

Table 1 Pore structure parameters of MSN and BR@MSN

Samples	Surface area (m^2/g)	Pore size (nm)	Pore volume (cm^3/g)
MSN	945.665	4.678	1.106
BR@MSN	925.723	4.289	0.993

Pore structure analysis

In fact, the loading of BR in MSN not only caused the variation in thermal stability, but also gave rise to the discrepancy in pore structure. The nitrogen adsorption–desorption isotherms and the pore size distributions of MSN and BR@MSN are shown in Fig. 2c, d, and the pore structure parameters are summarized in Table 1. Obviously, both of MSN and BR@MSN displayed type IV isotherms with H1 hysteresis loops according to the IUPAC classification (Fig. 2c), indicating that there were some slits in the structure [57]. In addition, MSN and BR@MSN exhibited mesoporous structures (Fig. 2d), and the average pore diameters of MSN and BR@MSN were 4.678 nm and 4.289 nm, respectively (Table 1). Smaller pore diameter of BR@MSN than MSN was attributed to the blocking effect derived from the loading of BR in

MSN occupied some space in mesopores. In addition, the BR loaded in MSN brought about the decrease in specific surface area and pore volume. Therefore, above results revealed the successful loading of BR in MSN, which was consistent with the results of TG analysis.

Morphology and particle size analysis

The morphology and the size of particles are of significance and closely relevant with their performance and application, especially in the field of nanotechnology [58, 59]. Figure 2e, f demonstrates the morphologies of MSN and BR@MSN, respectively. As shown in Fig. 2e, the particles size of MSN was about 110 nm. After loading BR, the particle size of BR@MSN slightly increased to about 120 nm (Fig. 2f). Obviously, both of MSN and BR@MSN nanoparticles were in a spherical shape. Besides, the hydrodynamic sizes of MSN and BR@MSN were also investigated, and the results revealed the corresponding sizes were 203 nm and 239 nm, respectively. Of note, compared with the hydrodynamic sizes obtained from the dynamic light scattering method, the particle sizes shown in SEM images were much smaller, which was mainly due to the swelling and slight aggregation of nanoparticles in aqueous solution for the hydrodynamic sizes [49].

Effects of BR concentration on seedling growth

As an endogenous plant growth regulator, BR plays an important role in regulating plant growth [60, 61]. In this work, the effects of BR, MSN, and BR@MSN with different concentrations (0.125 mg/L, 0.25 mg/L, 0.5 mg/L, 1.0 mg/L, and 2.0 mg/L, respectively) on the growth of cucumber seedlings were investigated, and the stem diameter and root length of the cucumber seedlings after being treated for 15 days are summarized in Fig. 3. It was found that the pristine cucumber seedlings exhibited little advantage in stem diameter and root length, while the applications of BR, MSN, and BR@MSN exerted obviously positive influence on the seedling growth. Specifically, as shown in Fig. 3a, similar stem diameters were found in the cucumber seedlings treated by BR and BR@MSN, while the application of MSN achieved the maximum enhancement in stem diameter. As we know, Si is able to deposit in the cell wall of plant stems, and thus strengthens the stem diameter to resist against biotic and abiotic stresses [62]. Because same mass of MSN and BR@MSN was applied, compared with BR@MSN, more Si element could be supplemented by MSN, thus leading to greater increase in stem diameter. As for the root length of cucumber seedling (Fig. 3b), after being treated by BR, the maximum root length (7.66 cm) was achieved at the concentration of 0.25 mg/L, while it decreased with the increase in BR concentration. When BR concentration reached 2.0 mg/L, the corresponding root length decreased to 4.45 cm. Above results revealed that, compared with low BR concentration, high BR concentration to some degree inhibited the root growth of cucumber seedlings. However, as for the cucumber seedlings treated by BR@MSN, even at the BR concentration of 2.0 mg/L, the root reached a high length of 8.10 cm, which increased by 82.02% compared with the ones treated by BR at the same concentration. This phenomenon was mainly attributed to the sustained release of BR from BR@MSN (described in the next section).

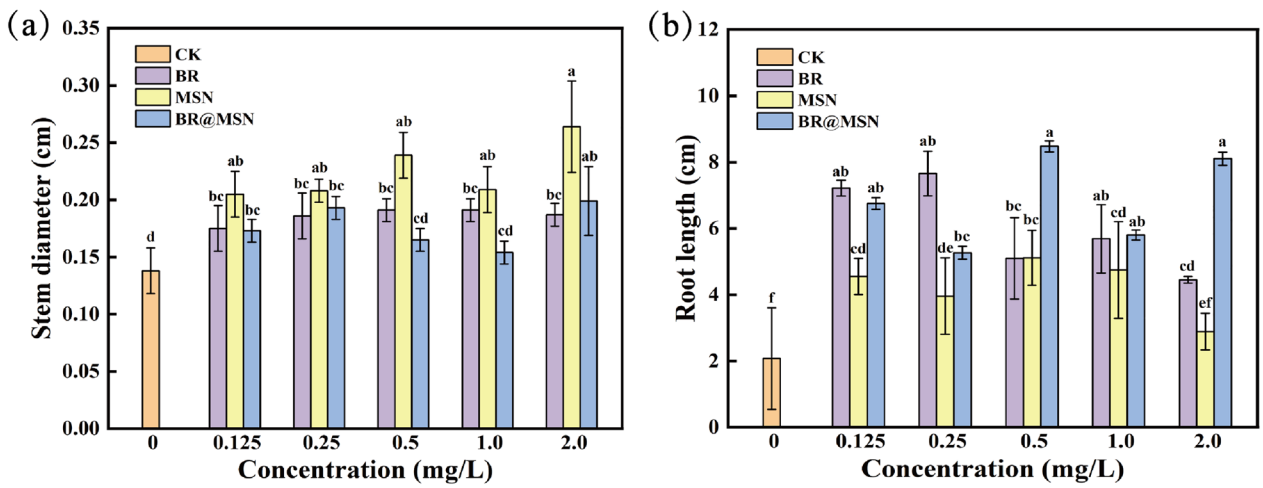

Fig. 3 Effects of BR, MSN, and BR@MSN with different concentrations on the **a** stem diameter and **b** root length of cucumber seedlings. The cucumber seedlings growing in the normal situation without salt stress. The same BR and BR@MSN concentration indicates they possess the same BR concentration, and the same MSN and BR@MSN concentration indicates they possess the same mass. The experimental data were measured three replicates. Different letters (a, b, c, d, e, f) indicate significant difference between treatments at $P \leq 0.05$

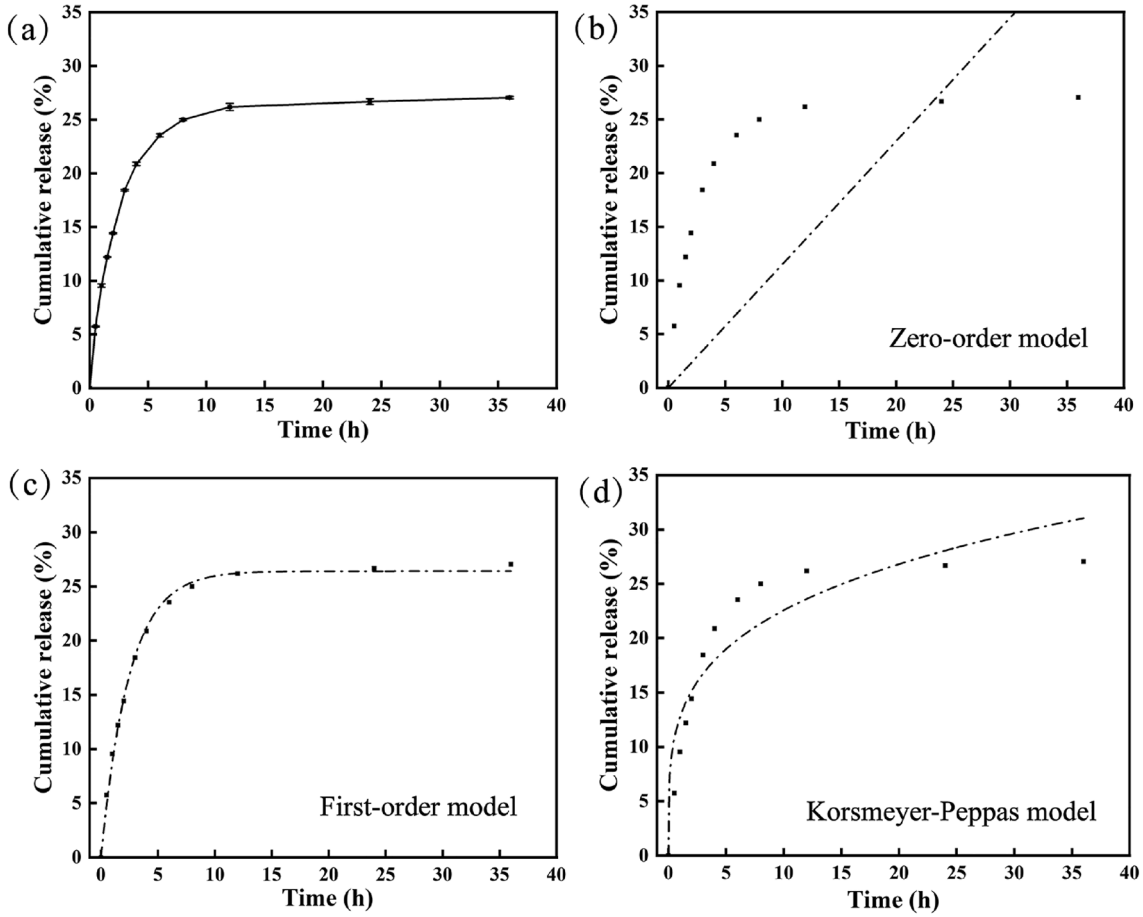

Fig. 4 **a** Cumulative release rates of BR from BR@MSN. **b** Zero-order, **c** first-order, and **d** Korsmeyer–Peppas fitting release curves of BR@MSN. Where the dots represent the original release curves, and the solid lines represent the fitting curves

Table 2 Release kinetic model fitting result of BR@MSN

Kinetic models	Fitting formula	Parameters		
		k_1	k_2	R^2
Zero-order model	$y=k_1t$	1.1487	–	0.5864
First-order model	$y=k_1[1-\exp(k_2t)]$	26.4167	0.4053	0.9970
Korsmeyer–Peppas model	$y=k_1t^{k2}$	12.7235	0.2488	0.8762
Higuchi model	$y=k_1t^{1/2}$	6.4769	–	0.1999
Hixson–Crowell model	$y=(k_2-k_1t)^3$	2.4989	−0.0180	0.3883

Sustained release behavior of BR from BR@MSN

As aforementioned, the discrepancy in the cucumber root lengths derived from the applications of BR and BR@MSN could be accounted for the sustained release of BR from BR@MSN. The sustained release behavior toward BR@MSN is demonstrated in Fig. 4a. Specifically, at the initial state, BR released rapidly from BR@MSN, which was mainly due to the fast dissolution of BR absorbed on MSN surfaces. Furthermore, because of the blocking effect caused by MSN and the interactions (hydrogen bonds, et al.) between MSN and BR, releasing tendency became relatively steady after 12 h. Such releasing tendency is similar to other research [63]. To further elucidate the release mechanism of BR from BR@MSN, five kinetic models (zero-order, first-order, Korsmeyer–Peppa, Higuchi, Hixson–Crowell) were used to fit the cumulative release curves, the fitting curves are shown in Fig. 4b–d and Additional file 1: Fig. S2, and the fitting results are summarized in Table 2. According to the regression coefficient (R^2) values of the kinetic fitting curves, the sustained release behaviors of BR from BR@MSN followed the first-order model, indicating the releasing behavior is closely relevant with the concentration gradient [64].

Of note, due to the sustained release property of BR@MSN, about 27% BR was released after continuously releasing for 36 h. Above results implied that the utilization of BR@MSN could effectively reduce the BR content exposed directly to cucumber seedlings, thus avoiding the inhibitory effect caused by high BR concentration. Therefore, at the same BR concentration of 2.0 mg/L, BR@MSN exerted more positive influence on seedling growth than the pure BR (Fig. 3b).

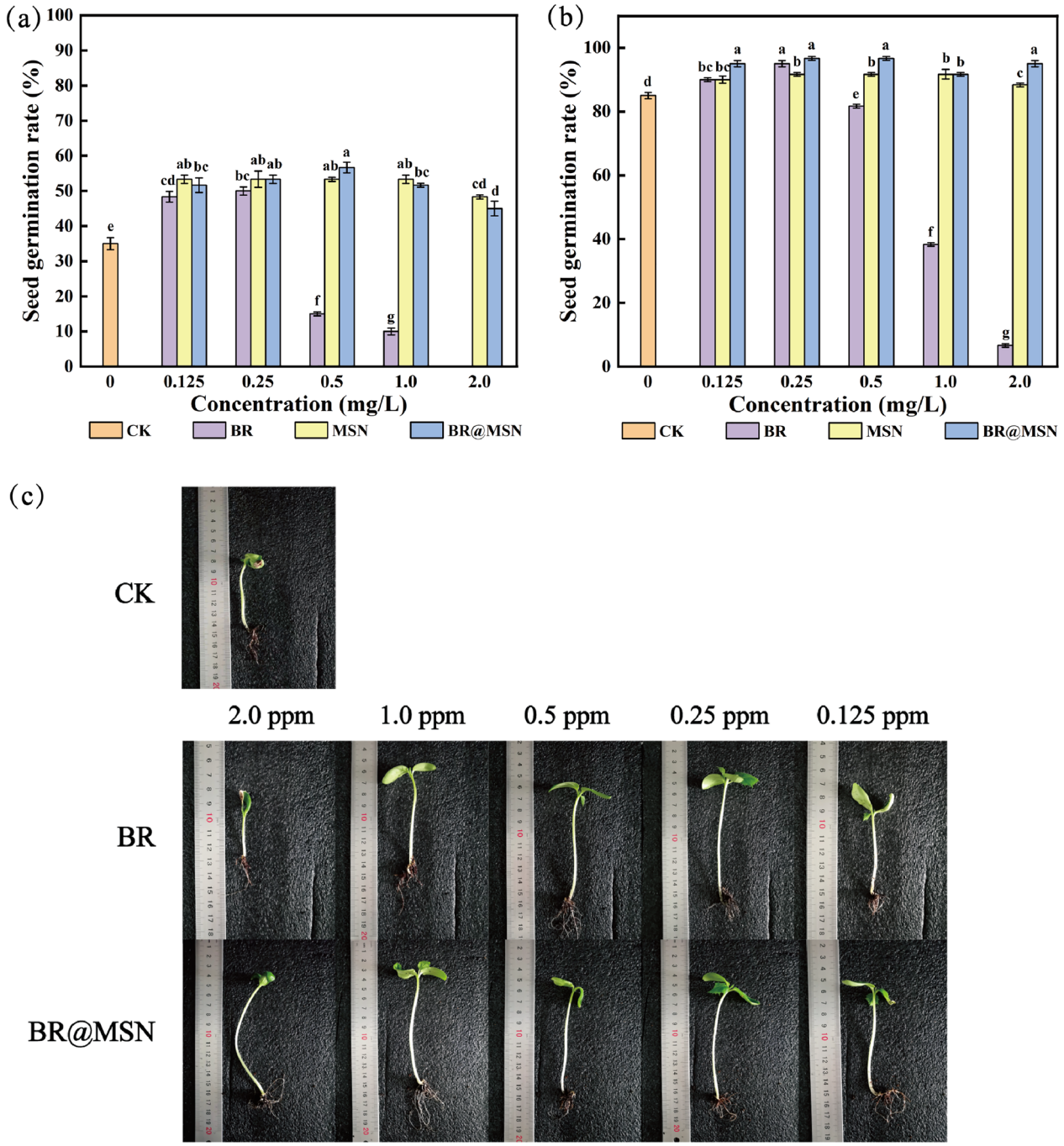

Fig. 5 Seed germination rates after being treated, respectively, by BR, MSN, and BR@MSN with different concentrations for **a** 3 days and **b** 5 days. **c** Growth status of the cucumber seedlings treated with different concentrations of BR and BR@MSN, respectively. CK represents the cucumber seed under salt stress without sample treatment. The experimental data were measured three replicates. Different letters (a, b, c, d, e, f, g) indicate significant difference between treatments at $P \leq 0.05$

Seed germination and seedling growth under salt stress

In fact, BR is not only able to regulate plant growth, but also alleviate the abiotic stress of plants, including the salt stress. The effects of BR@MSN with different concentrations on the seed germination and the seedling growth of cucumber plants under salt stress were investigated, and the results are demonstrated in Fig. 5. After the cucumber seeds under salt stress had been treated with BR for 3 days (Fig. 5a), it was found that higher BR concentration resulted in greater seed germination rate within the concentrations ranging from 0.125 mg/L to 0.25 mg/L. However, further increasing BR concentration above 0.25 mg/L, the seed germination rates were adversely decreased, indicating excessive application of BR inhibited seed germination. Of note, many reports revealed that nano silica could improve the salt resistance of plants and reduce the detrimental effect of salt stress to plant cells [47]. Experimental results in this work revealed the cucumber seeds treated with different MSN concentrations (from 0.125 mg/L to 2.0 mg/L) achieved little detrimental effect from salt stress. Instead, the application of MSN significantly improved the seed germination rate. As for BR@MSN, in the concentration range in this work, the germination rate of cucumber seed was also improved. Of note, although 0.5 mg/L BR inhibited seed germination, the same BR@MSN concentration demonstrated the best improvement in seed germination. This tendency was due to the collaboration of the alleviation of salt stress caused by MSN and the seed germination improvement resulted from the sustained release of BR from BR@MSN. As aforementioned, high BR concentration brought about the inhibition behavior toward seed germination. In the concentration of 1.0 mg/L and 2.0 mg/L, improvement behavior in seed germination rate could also be found for BR@MSN. At the same time, the excessive presence of BR from BR@MSN resulted in inferior effects for the seed germination rate than MSN, while the superior effects from MSN was mainly contributed to providing more Si element to resist against salt stress. After culturing for 5 days (Fig. 5b), similar phenomenon on seed germination rate could be found. High BR concentration (above 0.25 mg/L) inhibited the seed germination rate, while the applications of MSN and BR@MSN improve the seed germination rate even at high BR concentration (2.0 mg/L). Specifically, at the concentration of 2.0 mg/L, compared with BR, the application of BR@MSN resulted in the seed germination rate increased by 1324.29%. In addition, it was noteworthy that the application of BR@MSN achieved the dominant advantage in seed germination rate (increased by 11.76%), even greater than MSN. This phenomenon was mainly due to the steady and slow release of BR from BR@MSN avoiding excessive exposure of BR from BR@MSN to seedlings, combined with the alleviation effect derived from MSN toward salt stress, thus positively enhancing the seed germination rate.

Furthermore, the growth status of the cucumber seedlings under salt stress after being treated with BR and BR@MSN with different concentrations were observed and compared (Fig. 5c). The results were similar to the tendency of seed germination rate. Under salt stress, cucumber seedlings grew slowly with a relatively short stem. After being treated by BR at low concentration, the stem elongation of cucumber plants was promoted. However, increasing BR concentration adversely resulted in inhibitory effect. Of note, as for BR@MSN, due to the sustained release of BR from BR@MSN and the assistant resistance against salt stress provided by the nanocarriers, the stem elongation of cucumber seedlings increased along with BR@MSN concentration, indicative of the enhancement in salt stress resistance of cucumber seedlings.

Wetting ability on foliar surfaces

Wetting ability on foliar surfaces is a significant factor that should be considered for the applications of pesticides and plant hormones. Increasing wetting ability will reduce the losses from runoff, bouncing, and splashing of

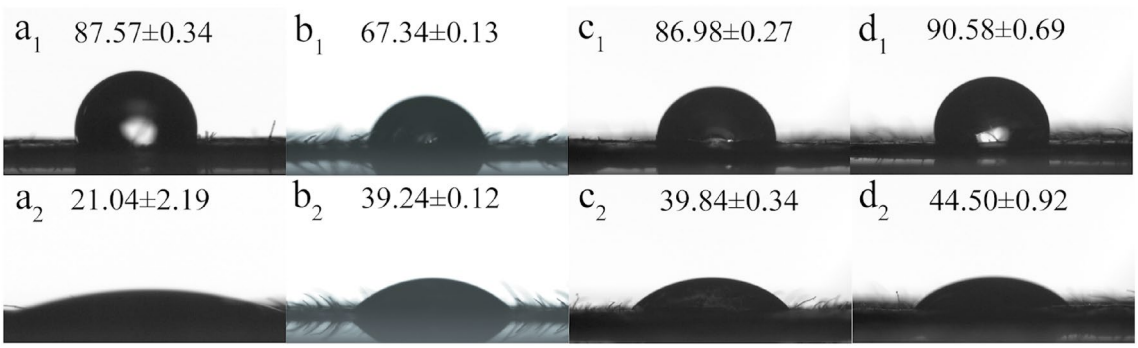

Fig. 6 Contact angles of $\mathbf{a}_1$ water, $\mathbf{b}_1$ BR, $\mathbf{c}_1$ MSN, and $\mathbf{d}_1$ BR@MSN. $\mathbf{a}_2$–$\mathbf{d}_2$ the samples with the addition of 0.05% Silwet L-77

droplets, and thus enhance the utilization [65]. As demonstrated in Fig. 6, due to the hydrophobic property of cucumber leaves, the contact angles of water, MSN, and BR@MSN droplets on foliar surfaces were around 90°. As for BR droplet, because ethanol was used for dissolution, the presence of ethanol decreased the contact angles to 67.34°. It is well-known that additives such as surfactants are commonly added to decrease the surface tension of droplets and increase the wettability on foliar surfaces. Silwet L-77 was reported as an effective surfactant with ability to solubilize cuticular waxes and enhance the hydration of cuticle [49]. In addition, 0.05% Silwet L-77 could significantly enhance the wettability of droplets on foliar surfaces. As demonstrated in Fig. 6, all contact angles on cucumber foliar surface are below 45° after the addition of Silwet L-77. As for BR@MSN droplet, with the assistance of Silwet L-77, the corresponding contact angle decreased from 90.58° to 44.5°, indicative of the enhancement in wettability on foliar surface.

Salt stress resistance analysis after the foliar application of BR@MSN

Remarkable wetting ability on foliar surfaces will facilitate the uptake of BR@MSN by plants, and we found that the foliar application of BR@MSN was able to enhance the salt stress resistance of cucumber seedlings. The discrepancy in salt stress resistance could be demonstrated by comparing the cell viability and superoxide anion (O_2^-) accumulation in cucumber seedlings. As shown in Fig. 7, compared with the normal cucumber leaves (CK_1), more uptake of Evans blue and Nitro blue tetrazolium (NBT) was found for the cucumber leaves under salt stress (CK_2), indicating the reduction in cell viability (Fig. 7a) and the augment in superoxide anion accumulation (Fig. 7b). After the foliar application of BR, the Evans blue staining and NBT staining became lighter at low concentration, while they turned to deeper after the increase in concentration, revealing low BR concentration was conducive to relieving salt stress. As for the foliar application of MSN, it was found that higher MSN concentration brought about greater resistance against salt stress. In the case of BR@MSN, Evans blue staining and NBT staining became lighter along with the concentration, and greater resistance against salt stress than MSN could be obviously found. This phenomenon was due to the collaboration of the alleviation effect from MSN and the sustained release of BR from BR@MSN to reduce the accumulation of reactive oxygen species and alleviate cell damage, thus promoting the cell viability of cucumber plants under salt stress.

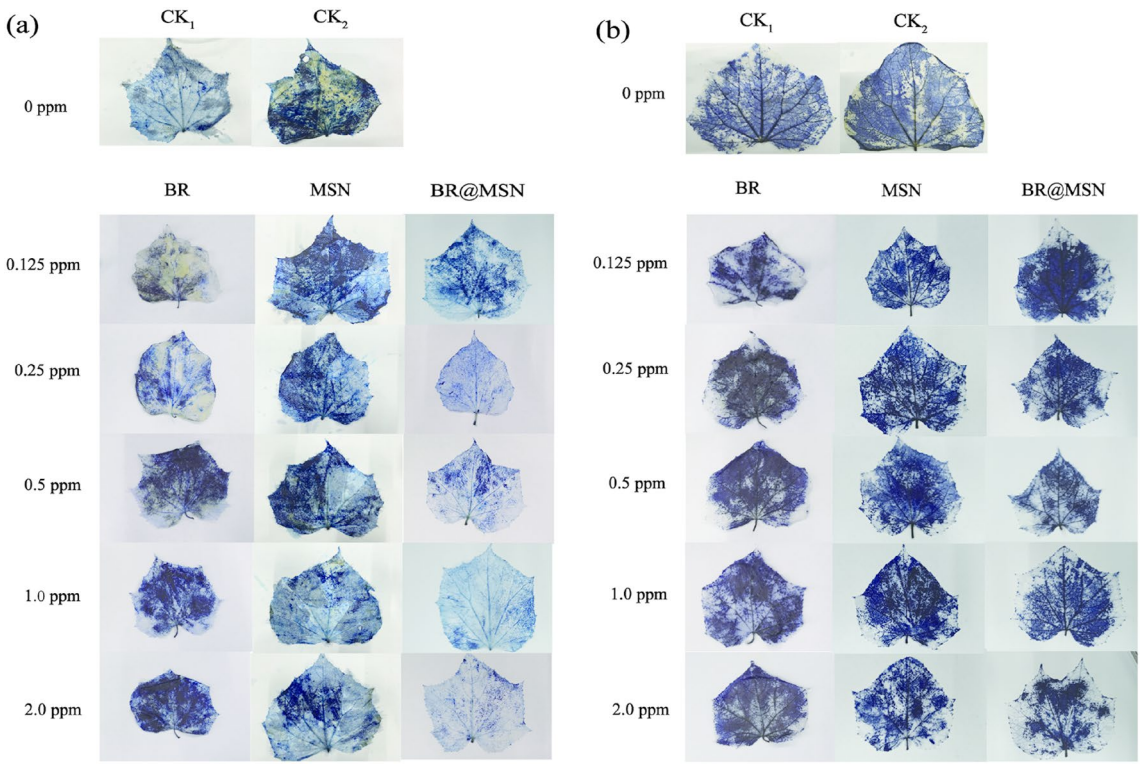

Fig. 7 Effects of BR, MSN, and BR@MSN with different concentrations on **a** cell viability and **b** superoxide anion accumulation of the cucumber leaves under salt stress. CK_1 represents the normal cucumber leaves, and CK_2 represents the cucumber leaves under salt stress without sample treatment

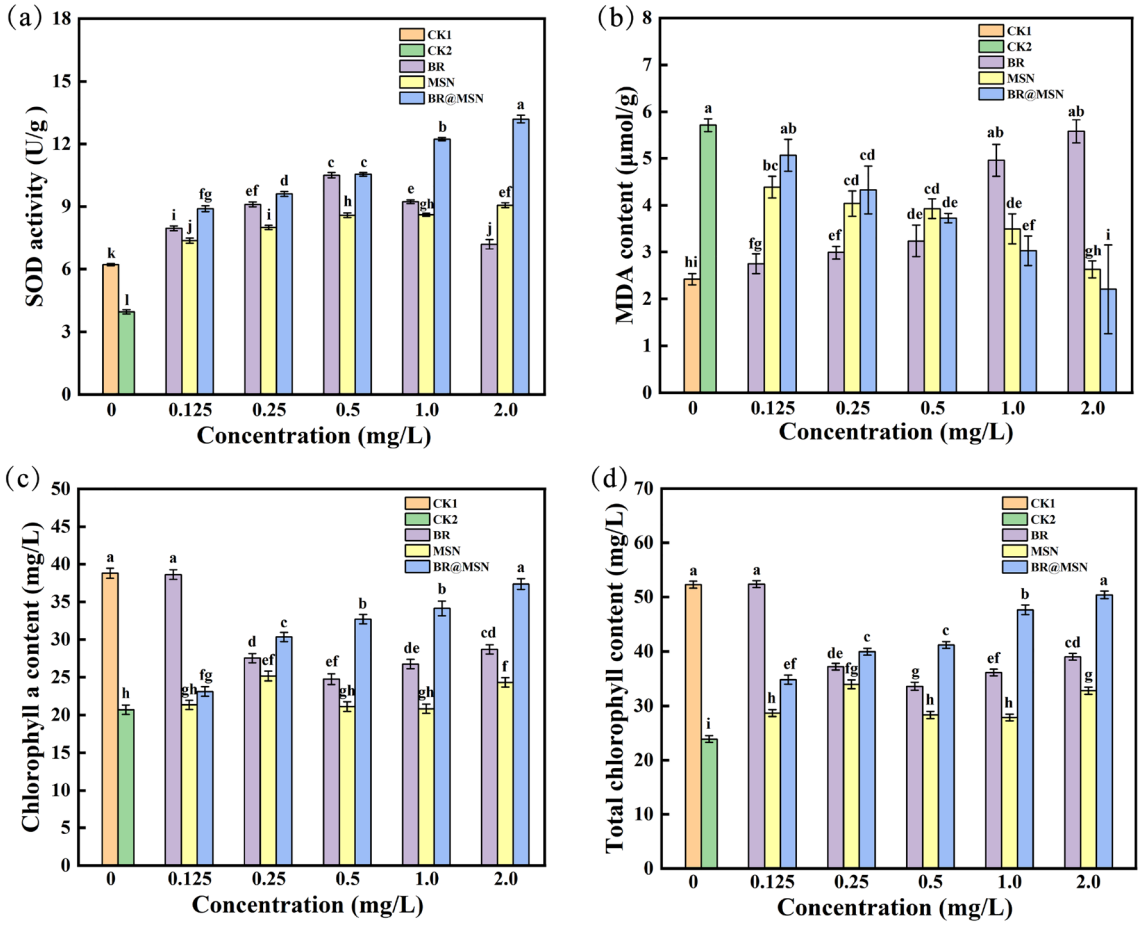

Fig. 8 (**a**) SOD activities, (**b**) MDA contents and (**c**, **d**) chlorophyll contents of the cucumber seedlings after foliar application of BR@MSN. CK_1 represents the normal cucumber seedling, and CK_2 represents the cucumber seedling under salt stress without sample treatment. The experimental data were measured three replicates. Different letters (a, b, c, d, e, f, g, h, i, j, k, l) indicate significant difference between treatments at $P \leq 0.05$

In addition, the enhancement in salt stress resistance benefited from the foliar application of BR@MSN could also be verified by the promotion in SOD activity, the decrease in MDA content, and the increase in chlorophyll contents as for the cucumber seedlings under salt stress. As we know, the improvement of antioxidant enzyme activity is beneficial to the enhancement in plant stress resistance [49]. As demonstrated in Fig. 8a, compared to the normal cucumber seedlings (CK_1), the SOD activity of the cucumber seedlings under salt stress (CK_2) decreased by 36.41%, indicative of the reduction in antioxidant enzyme activity. However, it was found that the foliar application of MSN increased the SOD activity of the cucumber seedlings under salt stress. Compared to CK_2, SOD activity increased by 129.51% after the foliar application of MSN at the concentration of 2.0 mg/L. Of note, under the same condition, experimental results revealed that the foliar application of BR@MSN significantly increased the SOD activity of the cucumber seedlings under salt stress even by 234.11%, indicating the reduction of SOD activity caused by salt stress in cucumber seedlings could be remarkably improved by BR@MSN.

As a product of membrane lipid peroxidation, MDA content is highly relevant with the growth status of plants and thus utilized to evaluate the level of salt stress. As demonstrated in Fig. 8b, the normal cucumber seedlings (CK_1) exhibited the lest MDA content of 2.42 μmol/g, while the MDA content increased significantly to 5.71 μmol/g as for the seedlings under salt stress (CK_2). Besides, increasing BR concentration from 0.125 mg/L to 2.0 mg/L led to the continuous increase of MDA content from 2.75 μmol/g to 5.58 μmol/g, indicating low BR content was conducive to the alleviation of salt stress. In addition, it was found that the foliar application of MSN resulted in the decrease of MDA content. Combined with the merit of MSN and the sustained release feature of BR@MSN, superior resistance against salt stress than MSN was found toward BR@MSN. When BR@MSN reached a high concentration of 2.0 mg/L, MDA

content decreased to 2.21 μmol/g, which was decreased by 61.30% compared to CK_2. In addition, the foliar application of BR@MSN brought about the increase in chlorophyll contents. Total chlorophyll content (Fig. 8d) is the sum of chlorophyll a content (Fig. 8c) and chlorophyll b content (Additional file 1: Fig. S3). Obviously, after the cucumber seedlings were suffered from salt stress, the total chlorophyll content decreased from 52.31 mg/L to 23.90 mg/L. Although the application of MSN to some degree increased the chlorophyll content, more significant increase was found toward BR@MSN. When BR@MSN concentration increased to 2.0 mg/L, the chlorophyll content increased by 110.88% compared with the cucumber seedlings under salt stress. Therefore, above results revealed the foliar application of BR@MSN could increase cell viability, alleviate superoxide anion accumulation, improve SOD activity, decrease MDA content, and protect chlorophyll, thus enhancing the salt stress resistance of cucumber seedlings.

Conclusions

In summary, this work developed a brassinolide sustained release agent system (BR@MSN) by loading BR to MSN nanocarrier to enhance the salt stress resistance of cucumber seeds and seedlings. The obtained BR@MSN possessed a particle size about 120 nm. Experimental results revealed that high BR concentration exerted inhibitory effect, while low BR content posed positive influence on seedling growth. Of note, BR@MSN demonstrated sustained release behavior that consistent with the first-order kinetic model, and such sustained release property avoided excessive exposure of BR to cause inhibitory effects. Due to the collaboration of the sustained release of BR from BR@MSN and the regulation enhancement from MSN, cucumber seed germination rate increased by 11.76% under saline condition, and it even increased by 1324.29% compared with the same BR concentration. In addition, these sustained release agents exhibited remarkable wetting ability on foliar surfaces, and the foliar application of BR@MSN significantly enhanced the salt stress resistance of cucumber seedlings by alleviating ROS accumulation and increasing the cell viability that could be confirmed by Evans blue staining and NBT staining experiments. In addition, after the foliar application of BR@MSN, SOD activity increased by 234.11%, MDA content decreased by 61.30%, and chlorophyll content increased by 110.88%, which further confirmed the improvement of cucumber seedlings against salt stress. Therefore, this work provides a facile approach to developing brassinolide sustained release agents, and the significant efficacy in enhancing salt stress resistance of cucumber seeds and seedlings makes them tremendously potential for agricultural applications to achieve sustainable agriculture.

Supplementary Information

The online version contains supplementary material available at https://doi.org/10.1186/s40538-023-00510-8.

Additional file 1: **Fig. S1.** DTG curves of BR, MSN, and BR@MSN. **Fig. S2** Higuchi and Hixson–Crowell fitting release curves of BR@MSN. **Fig. S3** Chlorophyll b content of the cucumber seedlings after foliar application of BR@MSN.

Acknowledgements
No applicable.

Author contributions
XZhong and RL proposed the concept and wrote the main manuscript. GS conducted the experiments, LH and HX analyzed the data, HZ and XZhou supervised and revised the manuscript. All authors reviewed the manuscript.

Funding
This work was supported by International Science and Technology Cooperation Project of Guangdong Province (Grant No. 2021A050530073), Innovation Team of Modern Agricultural Industry Technology System of Guangdong Province (Grant No. 2019KJ140), The Foundations of Guangdong Provincial Department of Education (2022ZDJS020), and Key Technologies R&D Program of Guangdong Province (2023B0202080002).

Availability of data and materials
All data generated or analysed during this study are included in this published article and its supplementary information files.

Declarations

Ethics approval and consent to participate
There are no ethical/legal conflicts to declare.

Consent for publication
All authors have read and approved the content and agreed to submit this paper for publication in your journal.

Competing interests
The authors declare that they have no competing interests.

Author details
[1]Key Laboratory of Green Prevention and Control On Fruits and Vegetables in South China of Ministry of Agriculture and Rural Affairs, Key Laboratory of Agricultural Green Fine Chemicals of Guangdong Higher Education Institution, School of Chemistry and Chemical Engineering, Zhongkai University of Agriculture and Engineering, Guangzhou 510225, Guangdong, People's Republic of China.

Received: 5 October 2023 Accepted: 21 November 2023
Published online: 01 December 2023

References

1. Mukhopadhyay R, Sarkar B, Jat HS, Sharma PC, Bolan NS. Soil salinity under climate change: challenges for sustainable agriculture and food security. J Environ Manage. 2021;280: 111736.
2. Rosa L. Adapting agriculture to climate change via sustainable irrigation: biophysical potentials and feedbacks. Environ Res Lett. 2022;17: 063008.
3. Mohammadi Alagoz S, Hadi H, Toorchi M, Andrzej Pawłowski T, Asgari Lajayer B, Price GW, et al. Morpho-physiological responses and growth indices of triticale to drought and salt stresses. Sci Rep. 2023;13:8896.

4. Hossain MS. Present scenario of global salt affected soils, its management and importance of salinity research. Int J Biol Sci. 2019;1:1–3.
5. Liu L, Wang B. Protection of halophytes and their uses for cultivation of saline-alkali soil in China. Biology. 2021;10:353.
6. Zhao S, Zhang Q, Liu M, Zhou H, Ma C, Wang P. Regulation of plant responses to salt stress. Int J Mol Sci. 2021;22:4609.
7. Latef AAHA, Alhmad MFAA, Kordrostami M, Abo-Baker AA, Zakir A. Inoculation with *Azospirillum lipoferum* or *Azotobacter chroococcum* reinforces maize growth by improving physiological activities under saline conditions. J Plant Growth Regul. 2020;39:1293–306.
8. Liu C, Mao B, Yuan D, Chu C, Duan M. Salt tolerance in rice: physiological responses and molecular mechanisms. Crop J. 2022;10:13–25.
9. Yang Y, Guo Y. Unraveling salt stress signaling in plants. J Integr Plant Biol. 2018;60:796–804.
10. Bayanati M, Mohammad Al-Tawaha AR, Bayanati M, Rasouli M, Asgari LB. Conferring drought and salinity stress tolerance in horticultural crops by Si application. SILICON. 2023;15:5833–43.
11. Ganapati RK, Naveed SA, Zafar S, Wang W, Xu J. Saline-alkali tolerance in rice: physiological response, molecular mechanism, and QTL identification and application to breeding. Rice Sci. 2022;29:412–34.
12. Hu L, Zhou K, Liu Y, Yang S, Zhang J, Gong X, et al. Overexpression of MdMIPS1 enhances salt tolerance by improving osmosis, ion balance, and antioxidant activity in transgenic apple. Plant Sci. 2020;301: 110654.
13. Aliyari Rad S, Dehghanian Z, Asgari Lajayer B, Nobaharan K, Astatkie T. Mitochondrial respiration and energy production under some abiotic stresses. J Plant Growth Regul. 2022;41:3285–99.
14. Khadem Moghadam N, Motesharezadeh B, Maali-Amiri R, Asgari Lajayer B, Astatkie T. Effects of potassium and zinc on physiology and chlorophyll fluorescence of two cultivars of canola grown under salinity stress. Arab J Geosci. 2020;13:771.
15. Zelm EV, Zhang Y, Testerink C. Salt tolerance mechanisms of plants. Annu Rev Plant Biol. 2020;71:403–33.
16. Fadiji AE, Yadav AN, Santoyo G, Babalola OO. Understanding the plant-microbe interactions in environments exposed to abiotic stresses: an overview. Microbiol Res. 2023;271: 127368.
17. Mallick PK. Evaluating potential importance of cucumber (*Cucumis sativus* L.-Cucurbitaceae): a brief review. Int J Appl Sci Biotechnol. 2022;10:12–5.
18. Rekha K, Thiruvengadam M. Secondary metabolite production in transgenic hairy root cultures of cucurbits. Transgenesis and secondary metabolism. 2017; 267–293.
19. Chen TW, Pineda IMG, Brand AM, Stützel H. Determining ion toxicity in cucumber under salinity stress. Agronomy. 2020;10:677.
20. Lan Y, Wu L, Wu M, Liu H, Gao Y, Zhang K, et al. Transcriptome analysis reveals key genes regulating signaling and metabolic pathways during the growth of moso bamboo (*Phyllostachys edulis*) shoots. Physiol Plantarum. 2021;172:91–105.
21. Ma F, An Z, Yue Q, Zhao C, Zhang S, Sun X, et al. Effects of brassinosteroids on cancer cells: a review. J Biochem Mol Toxic. 2022;36:23026.
22. Hu D, Wei L, Liao W. Brassinosteroids in plants: crosstalk with small-molecule compounds. Biomolecules. 2021;11:1800.
23. Manghwar H, Hussain A, Ali Q, Liu F. Brassinosteroids (BRs) role in plant development and coping with different stresses. Int J Mol Sci. 2022;23:1012.
24. Xiong CF, Bai YL, Yin XM, Ye TT. Use of chemical labeling-assisted liquid chromatography-mass spectrometry for discovering derivatives of brassinosteroids. J Chromatogr A. 2022;1685: 463639.
25. Dehghanian Z, Bandehagh A, Habibi K, Balilashaki K, Asgari Lajayer B. Impact of Abiotic Stress on Plant Brassinosteroids. Climate Change and the Microbiome. 2021; 63:279–298
26. She J, Han Z, Kim TW, Wang J, Cheng W, Chang J, et al. Structural insight into brassinosteroid perception by BRI1. Nature. 2011;474:472–6.
27. Mu D, Feng N, Zheng D, Zhou H, Liu L, Chen G, et al. Physiological mechanism of exogenous brassinolide alleviating salt stress injury in rice seedlings. Sci Rep. 2022;12:20439.
28. Li Y, Wu Y, Liao W, Hu L, Dawuda MM, Jin X, et al. Nitric oxide is involved in the brassinolide-induced adventitious root development in cucumber. BMC Plant Biol. 2020;20:102.
29. Sun Y, He Y, Irfan AR, Liu X, Yu Q, Zhang Q, et al. Exogenous brassinolide enhances the growth and cold resistance of maize (*Zea mays* L.) seedlings under chilling stress. Agronomy. 2020;10:488.
30. Ahammed GJ, Li X, Liu A, Chen S. Brassinosteroids in plant tolerance to abiotic stress. J Plant Growth Regul. 2020;39:1451–64.
31. Yaqoob U, Jan N, Raman PV, Siddique KM, John R. Crosstalk between brassinosteroid signaling, ROS signaling and phenylpropanoid pathway during abiotic stress in plants: does it exist? Plant Stress. 2022;4: 100075.
32. Wang S, Zhao H, Zhao L, Gu C, Na Y, Cheng S, Pan G. Application of brassinolide alleviates cold stress at the booting stage of rice. J Integr Agr. 2020;19:975–87.
33. Ji H, Yang B, Jing Y, Luo Y, Li B, Yan Y, et al. Trehalose and brassinolide enhance the signature ingredient accumulation and anti-oxidant activity in the hairy root cultures of *Polygala tenuifolia* Willd. Ind Crop Prod. 2023;196: 116521.
34. Kirtane AR, Verma M, Karandikar P, Furin J, Langer R, Traverso G. Nanotechnology approaches for global infectious diseases. Nat Nanotechnol. 2021;16:369–84.
35. Jin C, Wang K, Oppong-Gyebi A, Hu J. Application of nanotechnology in cancer diagnosis and therapy-a mini-review. Int J Med Sci. 2020;17:2964–73.
36. Shah MA, Pirzada BM, Price G, Shibiru AL, Qurashi A. Applications of nanotechnology in smart textile industry: a critical review. J Adv Res. 2022;38:55–75.
37. Malik S, Muhammad K, Waheed Y. Nanotechnology: a revolution in modern industry. Molecules. 2023;28:661.
38. Usman M, Farooq M, Wakeel A, Nawaz A, Cheema SA, Rehman H, et al. Nanotechnology in agriculture: current status, challenges and future opportunities. Sci Total Environ. 2020;721: 137778.
39. Arora S, Murmu G, Mukherjee K, Saha S, Maity D. A comprehensive overview of nanotechnology in sustainable agriculture. J Biotechnol. 2022;355:21–41.
40. Mubeen I, Mfarrej MFB, Razaq Z, Iqbal S, Naqvi SAH, Hakim F, et al. Nanopesticides in comparison with agrochemicals: outlook and future prospects for sustainable agriculture. Plant Physiol Bioch. 2023;198: 107670.
41. Zhong X, Gao F, Wei H, Zhou H, Zhou X. Functionalization of mesoporous silica as an effective composite carrier for essential oils with improved sustained release behavior and long-term antibacterial performance. Nanotechnology. 2022;33: 035706.
42. Ahmed H, Gomte SS, Prabakaran E, Prabakaran A, Agrawal M, Alexander A. Biomedical applications of mesoporous silica nanoparticles as a drug delivery carrier. J Drug Deliv Sci Tec. 2022;76: 103729.
43. Tang F, Li L, Chen D. Mesoporous silica nanoparticles: synthesis, biocompatibility and drug delivery. Adv Mater. 2012;24:1504–34.
44. Zhong X, Wen H, Zeng R, Deng H, Su G, Zhou H, et al. Zein-functionalized mesoporous silica as nanocarriers for nanopesticides with pH/enzyme dual responsive properties. Ind Crop Prod. 2022;188: 115716.
45. Shen Z, Wen H, Zhou H, Li H, Chen H, Zhou X. Coordination bonding-based polydopamine-modified mesoporous silica for sustained avermectin release. Mat Sci Eng C-Mater. 2019;105: 110073.
46. Zhao P, Cao L, Ma D, Zhou Z, Huang Q, Pan C. Translocation, distribution and degradation of prochloraz-loaded mesoporous silica nanoparticles in cucumber plants. Nanoscale. 2018;10:1798–806.
47. Ismail LM, Soliman MI, El-Aziz MHA, Abdel-Aziz HMM. Impact of silica ions and nano silica on growth and productivity of pea plants under salinity stress. Plants. 2022;11:494.
48. Attia EA, Elhawat N. Combined foliar and soil application of silica nanoparticles enhances the growth, ffowering period and ffower characteristics of marigold (*Tagetes erecta* L.). Sci Hortic. 2021;282: 110015.
49. Zhong X, Su G, Zeng Q, Li G, Xu H, Wu H, et al. Preparation of salicylic acid-functionalized nanopesticides and their applications in enhancing salt stress resistance. ACS Appl Mater Inter. 2023;15:43282–93.
50. Khan MAH, Baset Mia MA, Quddus MA, Sarker KK, Rahman M, Skalicky M, et al. Salinity-induced physiological changes in pea (*Pisum sativum* L.): germination rate, biomass accumulation, relative water content, seedling vigor and salt tolerance index. Plants. 2022;11:3493.
51. Li Y, Liu J, Fu C, Khan MN, Hu J, Zhao F, et al. CeO_2 nanoparticles modulate Cu-Zn superoxide dismutase and lipoxygenase-IV isozyme activities to alleviate membrane oxidative damage to improve rapeseed salt tolerance. Environ Sci: Nano. 2022;9:1116–32.
52. Zhang XH, Ma C, Zhang L, Su M, Wang J, Zheng S, et al. GR24-mediated enhancement of salt tolerance and roles of H_2O_2 and Ca^{2+} in regulating this enhancement in cucumber. J Plant Physiol. 2022;270: 153640.

53. Zhang LX, Chang QS, Hou XG, Wang JZ, Chen SD, Zhang QM, et al. The effect of high-temperature stress on the physiological indexes, chloroplast ultrastructure, and photosystems of two herbaceous peony cultivars. J Plant Growth Regul. 2023;42:1631–46.
54. Yan H, Hao L, Chen H, Zhou X, Ji H, Zhou H. Salicylic acid functionalized zein for improving plant stress resistance and as a nanopesticide carrier with enhanced anti-photolysis ability. J Nanobiotechnol. 2023;21(1):1–25.
55. Su G, Zhong X, Qiu S, Fan J, Zhou H, Zhou X. Preparation of mesoporous silica-based nanocomposites with synergistically antibacterial performance from nano-metal (oxide) and polydopamine. Nanotechnology. 2022;33: 155702.
56. Zhong X, Gao F, Lin H, Su G, Zhou H, Zhou X. One-pot self-assembly strategy to prepare mesoporous silica-based nanocomposites with enhanced and long-term antibacterial performance. Colloid Surface A. 2022;650: 129654.
57. Mohammadnezhad G, Soltani R, Abad S, Dinari M. A novel porous nanocomposite of aminated silica MCM-41 and nylon-6: isotherm, kinetic, and thermodynamic studies on adsorption of Cu (II) and Cd (II). J Appl Polym Sci. 2017;134:45383.
58. Mazayen ZM, Ghoneim AM, Elbatanony RS, Basalious EB, Bendas ER. Pharmaceutical nanotechnology: from the bench to the market. Futur J Pharm Sci. 2022;8:12.
59. Kong XP, Zhang BH, Wang J. Multiple roles of mesoporous silica in safe pesticide application by nanotechnology: a review. J Agr Food Chem. 2021;69:6735–54.
60. Zhang L, Song C, Guo D, Guo L, Hou X, Wang H. Identification of differentially expressed miRNAs and their target genes in response to brassinolide treatment on flowering of tree peony (*Paeonia ostii*). Plant Signal Behav. 2022;17:2056364.
61. Naveen N, Kumari N, Avtar R, Jattan M, Ahlawat S, Rani B, et al. Evaluation of effect of brassinolide in Brassica juncea leaves under drought stress in field conditions. Horticulturae. 2021;7:514.
62. Mandlik R, Thakral V, Raturi G, Shinde S, Nikolićet M, Triathi DK, et al. Significance of silicon uptake, transport, and deposition in plants. J Exp Bot. 2020;71:6703–18.
63. Hao L, Lin G, Chen C, Zhou H, Chen H, Zhou X. Phosphorylated zein as biodegradable and aqueous nanocarriers for pesticides with sustained-release and anti-UV properties. J Agr Food Chem. 2019;67:9989–99.
64. Lai H, Chen S, Su X, Huang X, Zheng Q, Yang M, et al. Sponge-liked silica nanoporous particles for sustaining release and long-term antibacterial activity of natural essential oil. Molecules. 2023;28:594.
65. Xu X, Cao L, Cao C, Chen H, Zhang H, Li Y, et al. Fungicide itself as a trigger to facilely construct Hymexazol-Encapsulated polysaccharide supramolecular hydrogels with controllable rheological properties and reduced environmental risks. Chem Eng J. 2023;452: 139195.

Publisher's Note